

THE OIL SEEPAGE INDEX MAP

TECHNICAL INFORMATION



TABLE OF CONTENTS

01. Context

Technology evolution
in detecting oil seeps

02. Methodology

Understand each step
from space to the map

03. Validation

Comparing the map to
geochemical samples

04. Conclusion

Contributions from the
Oil Seepage Index Map

05. References

Sources mentioned



Context

Hydrocarbons seepage has been used since the early days of the oil industry as an important exploration tool. It indicates both the presence of source rocks and the occurrence of geological processes of thermal maturation and migration of the oil. In offshore areas, however, the high costs of sediment sampling campaigns limit direct evidence measurements of seepage. Thus, despite the enormous potential of oil seeps to enhance petroleum systems assessment and risk analysis of plays and prospects, their use, especially for ultra-deep regions, is still relatively restricted.

One of the strategies to reduce this limitation is to remotely retrieve information. The remote study of oil seeps, until the mid-2000s, focused exclusively on detecting slicks on the sea surface using satellite imagery.

Synthetic Aperture Radar (SAR) images can detect oil because it dampens the ocean surface capillary waves. This sort of detection has been widely validated (MacDonald et al., 1996; Scantland and Biegert, 1996; Biegert et al., 1997; Willians and Laurance, 2002; Miranda et al., 2004).

But the position of the oil on the sea surface can be very far from its origin on the ocean bottom, due to the action of winds and ocean currents. For exploration purposes, the location of the oil source on the seabed is the only way to connect seep information to the geological context.

Since the decade of 2010, computational models have been used to simulate the ocean circulation and the oil trajectory back in time and space to find its origin on the sea bottom (Mano et al., 2011; 2014; 2016).

The inverse modeling technology is now used to generate an oil seepage index map: a regular grid whose cells have values from 0 to 1, indicating the potential for oil seeping at that point. This way one can quantify the chances of natural oil seepage on the seafloor using only remote technologies. Very important information for exploration risk analysis and/or for the calibration/assessment of petroleum systems models.



Methodology

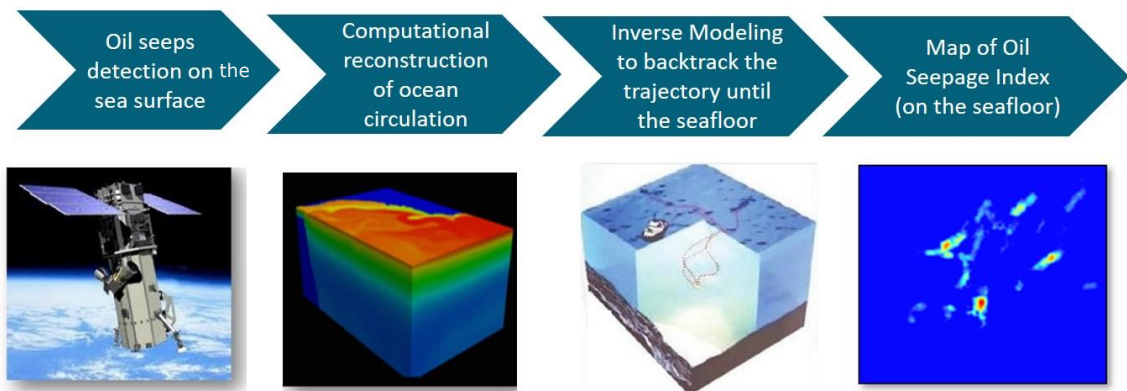


Figure 1 The four steps of the methodology

To make a clear difference between the two levels of information (sea surface and bottom), we name the oil slick detected by a satellite on the sea surface as “seep” and the regions on the seabed where oil leaks occur, identified by the inverse modeling, as “seep regions”.

The methodology to identify the oil seep regions on the seafloor using only remote technologies takes four steps (Figure 1):

- (1) detection of oil seeps on the sea surface;
- (2) computational reconstruction of ocean circulation;
- (3) inverse modeling of oil seep trajectories and
- (4) map generation of oil seepage index on the seafloor level.



Methodology

STEP 1

Oil seeps detection on the sea surface

The oil dampens the ocean surface capillary waves, smoothing the sea surface. This roughness difference between oil and water can be captured by SAR. SAR systems can screen large areas, with a high spatial resolution, operating night and day and getting data under any meteorological conditions.

One of the main advantages of satellite detection is precisely the coverage area. A single image can cover about 100,000 km², allowing a regional view of the seepage dynamics.

However, satellite detection is only possible for regions that are imaged when the seep is on the sea surface. Thus, the greater the number of available images, the greater the chances of detecting seeps.

The number of images may vary according to the geological characteristics and the migration dynamics in the studied region. As the oil leaks from the seafloor in pulses, in regions where the pulse frequency is greater, fewer images are needed to detect seeps.

For each SAR image, a textural classification algorithm extracts the features that are indicative of seepage slicks on the sea surface. After that, it uses environmental data, geometric parameters of the feature and its distance to vessels and platforms to classify each slick into seep, spill or false-target. Only the slicks classified as seep go step 3 to be modeled.

OilFinder has participated in the longest Project of validating the classification of seeps led by Pemex, Radarsat and Federal University of Rio de Janeiro. For 13 years, more than 12,000 oil features were detected by SAR images in the Gulf of Mexico, and then classified and checked in-situ by a Pemex team.



Methodology

STEP 2

The oceanic circulation

To start simulating the displacement of the oil in the marine environment we need to reconstruct the oceanic dynamics at the time of oil detection and in the previous days. This is what hydrodynamic modeling does, simulating the oceanic current field, using the physical principles related to the conservation of momentum, energy and mass.

These principles can be expressed in mathematical equations, in a system where the main unknowns are the horizontal components of current velocity, in different vertical layers. The solution of this system of equations delivers a “cube” of ocean current data, simulating the oceanic circulation for a given region.

The HYCOM - HYbrid Coordinate Ocean Model (Halliwell et al., 1998; 2000; Bleck, 2002) – was the chosen model. The sea surface height, temperature and wind data from satellites are assimilated into the model (Figure 2). Statistic correlations are used to extrapolate the sea surface information throughout the water column, making the whole cube close to the real ocean. The hydrodynamic simulation assimilates wind data every 6 hours and sea surface temperature and elevation every 24 hours. Outputs of ocean currents are on an hourly basis.

In the end, the ocean circulation of each date with seep detection is reconstructed, so that each seep detected is associated with a 4D oceanic circulation and a wind field, reproducing the same current conditions of the detection date.

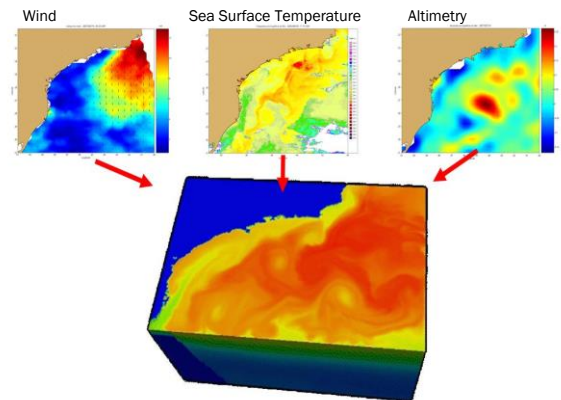


Fig. 2 4D hydrodynamic reconstruction method with data assimilation of wind, sea surface temperature and altimetry.



Methodology

STEP 3

The oil backward trajectory until the seafloor

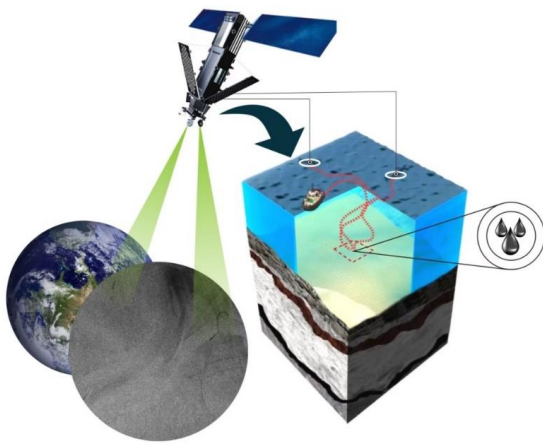


Fig. 3: Illustrative scheme of the inverse modeling, with the backward trajectory of the seeps until the bottom, after they are detected by satellite.

SAR images enable the detection of oil slicks, but only on the sea surface. And it is not enough to estimate its origin on the ocean floor. So, the inverse modeling goes back in time and space to estimate the oil path between the position on the sea surface where the satellite detected it, and the region where the oil has leaked, on the bottom (Figure 3).

Inverse Modelling imports and inverts the wind and 4D current fields obtained in the previous step. It also imports bathymetry and seep data (date, time and position).

Then, for each seep, the model performs tens of deterministic computational simulations of the oil backward displacement in a three-dimensional Cartesian domain (from the surface to the seabed), slightly varying key input parameters.



Methodology

STEP 4

The Oil Seepage Index Map

After plotting all the solutions on the seafloor of each seep on a regular grid with a spatial resolution of $(1/40)^0$, an algorithm starts scanning the grid, looking for cells with a high density of solutions. If a grid window of 3x3 presents more than 2 solutions of different seeps, then the central cell of the window is mapped as a cluster.

If a cell is not a cluster, its score is zero. For the other cases, cells are scored from 0 to 1, according to the following parameters:

- Number of solutions of different seeps in the cluster
- Number of solutions of the same seep in different clusters
- Number of different detection dates
- Distance from the seeps to the cluster

The final map, therefore, is no longer considering only single cases of converging deterministic solutions and become a raster that computes hundreds of solutions, weighted by intelligent algorithms. Figure 4 presents a real example of the Oil Seepage Index Map.

The index is dynamic and can change with a new satellite image. A new seep detected may influence the index as new seep regions can be mapped and/or the score of regions already mapped can get higher. Therefore, the greater the number of SAR images, the more reliable the index.

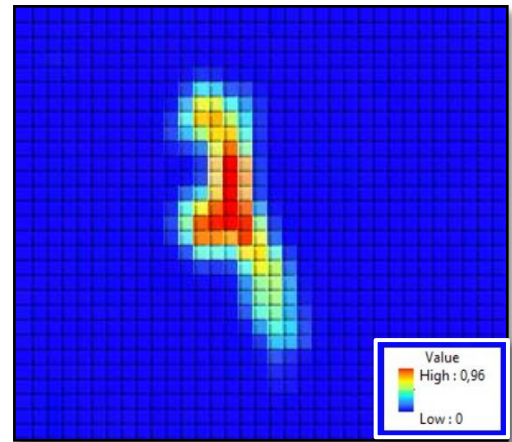


Fig. 4: Example of the Oil Seepage Index Map in a region with proven natural seepage. The red tones indicate a greater probability of oil seeping on the seafloor.



Validation

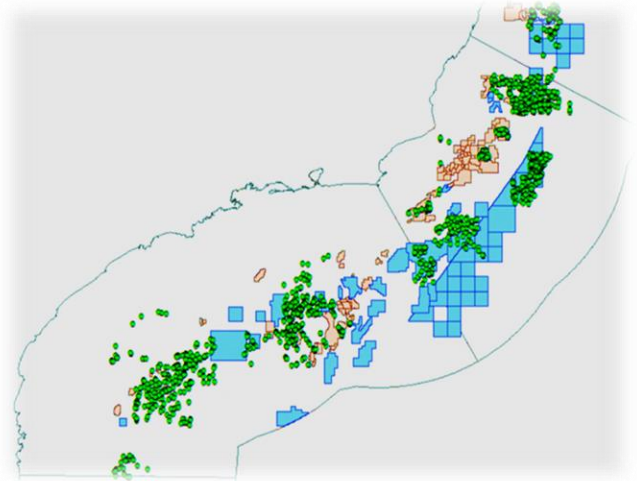


Fig. 5: The area of interest in the validation study. Green dots indicate the location of the 1,310 piston cores used in the Oil Seepage Index validation. Blue polygons are exploratory blocks and orange ones are oil fields

The study area for the validation of the Oil Seepage Index was the Brazilian Southeastern Margin (Santos, Campos and Espirito Santo Basins) (Figure 5). The region concentrates the largest oil reserves and the largest producing fields in Brazil.

On one hand, it presents a higher availability of satellite data, the input for the inverse modeling technology. On the other hand, there is also a great amount of geochemical analysis of bottom samples, necessary to validate the methodology.

In meteo-oceanographic terms, although the region presents a dominant NE wind condition and a southwestward current (Brazil Current), these characteristics are often disturbed by the presence of cold fronts, eddies and currents with opposite directions throughout the depth. Due to these characteristics, the origin of the seepage on the seafloor can be in a radius of tens of km and in any direction from the seep detected on the sea surface, which is also a good condition to test the method.

To generate the Oil Seepage Index Map, we used a database of 754 seeps on the sea surface, detected by different satellites (ERS-1/2, Radarsat-1/2, Envisat, Sentinel), between 1996 and 2019 at Santos, Campos and Espirito Santo basins. An algorithm scanned the grid to identify the cells that are the relative maximums. A relative maximum is a cell with an index greater than 0.25, which also presented the highest score within a 5x5 window, being the analyzed cell the center of the window.

Then we compared the oil seepage index map to the geochemical results of sediment samples collected in 1,310 piston cores. They were collected by Geochemical Solutions International Inc., between 1998 and 2000. Fig. 5 shows the position of the cores.



Validation

Two sediment samples of each core were analyzed using 3 different screen techniques:

- TSF (Total Scanning Fluorescence) - Increasing fluorescence generally corresponds to greater petroleum concentrations in samples;
- UCM (Unresolved Complex Mixture of hydrocarbons) - UCM concentrations provide an estimate of total extractable hydrocarbons and are an important seep indicator;
- Headspace gas (C2-C4) - headspace gas concentrations of C2-C4 components (ethane through butane) are frequently high at sites of hydrocarbon seeps.

Following Bernard et al.(2008), the results of TSF, UCM and C2C4 were plotted for all samples to define regional thresholds for their backgrounds. Anomalies of TSF and UCM indicate the presence of liquid hydrocarbon (HC) and anomalies of C2C4 indicate the presence of gaseous HC. For validation purposes, anomalous values for liquid or gas were considered as HC evidence.

The cores were divided into 2 classes (with HC and without HC) and plotted on the same grid of the Oil Seepage Index Map. Then the cells containing only cores without HC were labeled as without HC. The cells with at least one core with HC were labeled as with HC. The ones with no cores were excluded from the analysis.

Considering all cells with a core, the success rate (the percentage of cells with HC over the total of cells with cores) was 30.0%.



Validation

The validation consisted of comparing this performance with the percentages obtained around the relative maximum cells. That is, among the cells that contained at least one core, only the relative maximums or the ones up to 2 cells away from a relative maximum were analyzed. This way, the success rates were measured in the relative maximum cells and in the cells within 3x3 and 5x5 windows, where a maximum relative is the center cell. Table 1 shows the results.

Table 1: Comparing the success rates of all cells with cores and the cells close to relative maximums of the Oil Seepage Index. The relative maximum cells (1x1) and also the 5x5 and 3x3 windows centered on relative maximum cells were considered.

	All cells with cores	Windows centered on relative maximum cells		
		5x5	3x3	1x1
Success rate	30.0%	34.1%	47.2%	50.0%
Performance Improvement		13.7%	57.5%	66.8%

There is a progressive improvement in the performance of the cores (compared to all cells with cores) as they approach the relative maximums of the Oil Seepage Index. It means there is an increased performance from a 5x5 window to a 1x1 window. In other words, if only cores close to relative maximums of the Oil Seepage Index were collected, their success rates would be higher. Considering only the relative maximum cells (1x1), the performance would be 67% better, confirming the potential of the methodology in increasing the ability to find seep regions on the seafloor.



Conclusion

The oil industry began by following evidence of oil seeping on the ground. However, as exploration has increasingly moved in the offshore direction, it was no longer possible to "see" the ground due to the water column. Also, in-situ data collection campaigns are expensive and restricted to a local scale. The result was the loss of the protagonism of oil seeps in the exploration process.

Building the Oil Seepage Index Map may contribute to bring back the protagonism of oil seeps as it:

- (1) spatially quantifies the probability of occurrence of natural oil seepage on the seafloor, making this information easier to assimilate in risk analysis models or petroleum systems models;
- (2) uses only remote technologies, reducing the costs and risks of research; and
- (3) maps an extensive area, enabling a regional interpretation of the results.

The results of the Oil Seepage Index Map were validated by geochemical data from sediment samples. More than 1,300 piston cores were used in this validation.

Sediment samples collected close to relative maximums of the Oil Seepage Index presented success rates 67% higher than the total set of samples.



References

1. Bernard, B. B., J.M. Brooks, P. Baillie, J. Decker, P.A. Teas and D.L. Orange, 2008: Surface Geochemical Exploration and Heat Flow Surveys in Fifteen (15) Frontier Indonesian Basins. Proceedings, Indonesia Petroleum Association, Thirty-Second Annual Convention & Exhibition, May 2008.
2. Biegert, E.K., R.N. Baker, J.L. Berry, S. Mott and S. Scantland, 1997: Gulf Offshore Satellite Applications Project detects oil slicks using Radarsat. Proceedings of the International Symposium Geomatics in the Era of RADARSAT (GER'97), Ottawa, Canada, May 1997.
3. Bleck, R., 2002: An oceanic general circulation model framed in hybrid isopycnic-Cartesian coordinates. *Ocean Modeling*, 4, 55-88.
4. Halliwell, G. R., Jr., R. Bleck, and E. Chassignet, 1998: Atlantic Ocean simulations performed using a new hybrid-coordinate ocean model. EOS, Fall 1998 AGU Meeting.
5. Halliwell, G. R., R. Bleck, E. P. Chassignet, and L.T. Smith, 2000: Mixed layer model validation in Atlantic Ocean simulations using the Hybrid Coordinate Ocean Model (HYCOM). EOS, 80, OS304.
6. MacDonald, I.R., J.F. Reilly, Jr., S.E. Best, R. Venkataramaiah, R. Sassen, N.L. Guinasso, Jr., and J. Amos, 1996: Remote sensing inventory of active oil seeps and chemosynthetic communities in the northern Gulf of Mexico: in D. Schumaker and M. A. Abrams, eds., *Hydrocarbon migration and its near-surface expression: AAPG Memoir 66*, p. 27-37.
7. Mano, M.F., C. Beisl, and L. Landau, 2011: Identifying Oil Seep Areas at Seafloor Using Inverse Modeling. Extended Abstract, AAPG International Conference & Exhibition, Milan.
8. Mano, M.F., C. Beisl, C.Y.S Siqueira, and J.S. Pereira, 2014: Evaluation of remote technologies applied to natural seep mapping and their impact in oil exploration. Rio Oil & Gas Conference. Rio de Janeiro, Brazil.
9. Mano, M.F., C. Beisl and C. Soares, 2016: Oil seeps on the seafloor of Perdido, Mexico. Extended Abstract, AAPG International Conference & Exhibition, Cancún.
10. Miranda, F.P., A.M.Q. Marmol, E.C. Pedroso, C.H. Beisl, P. Welgan, and L.M. Morales, 2004: Analysis of RADARSAT-1 data for offshore monitoring activities in the Cantarell Complex, Gulf of Mexico, using the unsupervised semivariogram textural classifier (USTC). *Canadian Journal of Remote Sensing*, v. 30/3, p. 424-436.
11. Scantland, S., and E.K. Biegert, 1996: Radar locates offshore oil slicks. *Earth Observation Magazine*, v. 5, p. 30-32.
12. Willians, S.A., and G. Laurence, 2002: The role of satellite seep detection in exploring the South Atlantic's ultradeep water: in *Surface Exploration Case Histories. Applications of Geochemistry, Magnetism and Remote Sensing*. D. Schumacher and L.A. Le Schack, eds., AAPG Studies in Geology No. 48 and SEG Geophysical References Series No. 11, p. 327-344.

Thank you



oilfinder@globaloilfinder.com

www.globaloilfinder.com